Proceedings of the 11th World Congress on Mechanical, Chemical, and Material Engineering (MCM'25)

Barcelona, Spain -Paris, France - August, 2025

Paper No. HTFF 117 DOI: 10.11159/htff25.117

Design and Numerical Analysis a SAR ' $(Y-T)_{\alpha}$ ' Micromixer

Md Readul Mahmud¹, Asma Begum¹, Farhad Alam¹

¹Department of Physical Sciences, Independent University, Bangladesh (IUB) Plot 16 Block B, Aftabuddin Ahmed Road Bashundhara R/A, Dhaka-1245, Bangladesh mahmud.readul@iub.edu.bd; ablipi@iub.edu.bd; farhad@iub.edu.bd

Abstract - A novel split-and-recombined (SAR) ' $(Y-T)_{\alpha}$ ' micromixer is designed and analyzed numerically. The proposed micromixer is composed of four identical elements that are connected by angles α and β . The value of alpha (α) is varied from 0° to 90° and the value of beta (β) is always kept constant ($\beta=0^{\circ}$) to analyze the effect on the SAR process and mixing performance for Reynolds numbers from 1 to 100. The numerical data shows that the SAR process strongly depends on the connecting angle α ; at the mid-range of Reynolds numbers ($40 \le Re < 80$) mixer ($Y-T)_{45^{\circ}}$ shows the highest efficiency (about 90%) whereas ($Y-T)_{75^{\circ}}$ and ($Y-T)_{90^{\circ}}$ mixers yield more than 93% efficiency at higher Reynolds numbers ($80 \le Re \le 100$). Mixer ($Y-T)_{0^{\circ}}$ ($\alpha=0^{\circ}$) displays the lowest efficiency among all five examined mixers which is less than 50% at Re > 10. The mixing efficiency also varies with the number of elements and Reynolds numbers. The proposed mixer has a significantly lower mixing energy cost (MEC) when compared with a well-known Tear-drop mixer. In addition, the split-and-recombined process, the influence of secondary flow, and pressure drop characteristics at various Reynolds numbers are presented and discussed.

Keywords: CFD, Efficiency, Mixing energy cost (MEC), Pressure drop, SAR

1. Introduction

Numerous numerical and experimental assessments have been performed to improve the mixing quality of two fluids utilizing active and passive techniques [1]. Microfluidic systems play an important role in various applications such as environmental science, chemical processes, biochemistry, biological reactions, medication discovery and distribution, medical diagnosis, drug delivery, chemical synthesis, and the food industry, etc. [2]. Microfluidic systems possess many advantages such as Rapid analysis, mobility, greater control, cheap cost, fast throughput, and spending fewer quantities of expensive reagents [3]. In addition, microfluidics has unique properties, such as high surface area to volume ratios and rapid mass and heat transfer, which have paved the way for innovations in a variety of scientific and commercial fields, promising increased efficiency, portability, and cost-effectiveness in a wide range of applications. Flow fluid within micromixers often occurs in laminar conditions with smaller Reynolds numbers due to their small size, high-pressure needs, and material sensitivity. Mixing in microchannels is mostly governed by molecular diffusion, an insufficient and useless process [4]. Moreover, the extensive literature shows a wide categorization of microfluidics micromixers into two major types, active and passive micromixers, based on the external energy supply to operate [5]. Active micromixers rely on external energy sources such as electric field, pressure field, thermal field, magnetic field, and acoustic field or pulsating low to perturb the fluid flow [6].

In this paper, a ' $(Y-T)_{\alpha}$ ' split-and-recombined micromixer containing four elements was proposed. The effect of the connecting angle ' α ' between two elements on the mixing performance of the micromixer was simulated ($1 \le Re \le 100$) and the fluid flow pattern and mixing mechanism were studied using ANSYS 15 software. The proposed micromixers were assessed by computing the Mixing Index (MI), Mixing Energy Cost (MEC), and the associated pressure drop.

2. Micromixer Design

A novel 3D split and recombined ' $(Y - T)_{\alpha}$ ' mixer is proposed that is composed of 4 identical elements; each element is made of one 'Y' and one 'T' shaped part as shown in Figure 1. The length of one element is 4 mm and the height of the mixers is always kept at 0.4 mm.

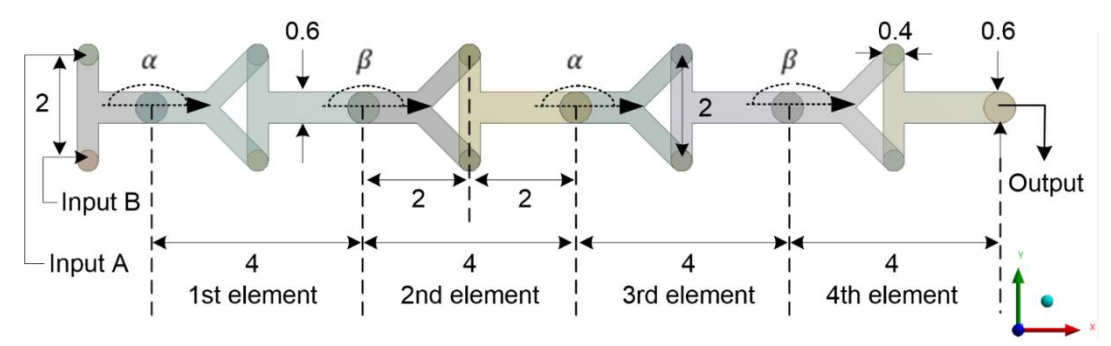


Fig. 1: Top view of the ' $(Y - T)_{\alpha}$ ' micromixer (all the dimensions are in mm).

The proposed ' $(Y - T)_{\alpha}$ ' mixers' four elements are connected by angles α and β ; the value of angle α is changed from 0° to 90° ; increased by 15° each time and angle β is always kept constant with a value of 0° . Therefore, five ' $(Y - H)_{\alpha}$ ' mixers are represented by $(Y-T)_{0^{\circ}}(\alpha=0^{\circ})$, $(Y-T)_{30^{\circ}}(\alpha=30^{\circ})$, $(Y-T)_{45^{\circ}}(\alpha=45^{\circ})$, $(Y-T)_{75^{\circ}}(\alpha=75^{\circ})$, and $(Y-T)_{90^{\circ}}$ ($\alpha=90^{\circ}$). Figure 2 represents the side view of $(Y-T)_{\alpha}$ mixer for $\alpha=45^{\circ}$.

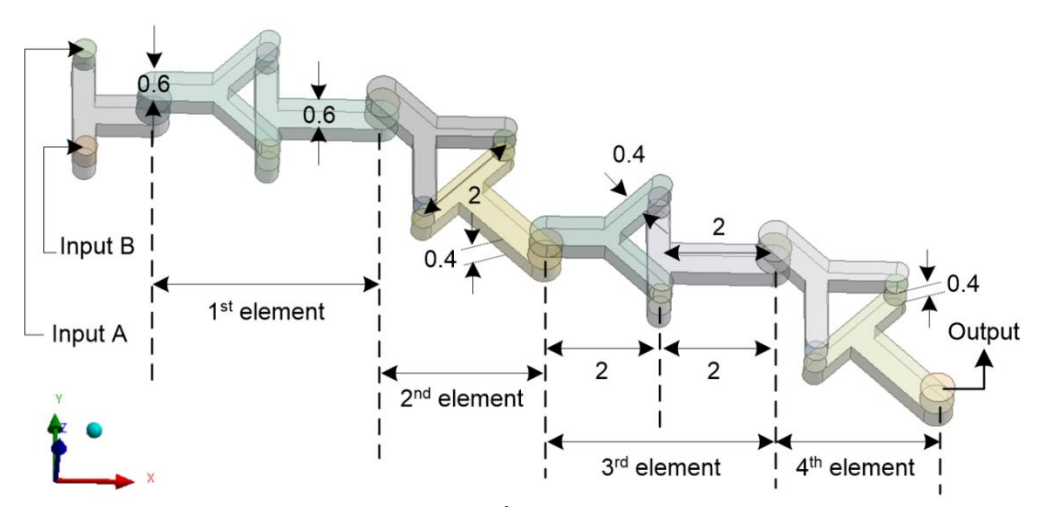


Fig. 2: Diagram of the $(Y - T)_{45}$ ° $(\alpha = 45^\circ)$ micromixer (all the dimensions are in mm).

3. Numerical Method and Mesh Independency Study

In this research, the mixing performance and pressure loss of the micromixer are first analyzed by numerical simulation using the ANSYS Fluent 15. The governing equations include the 3D Navier-Stokes equation, the continuity equation, and a species convection-diffusion equation. Since the flow is laminar, the following equations are employed [7].

$$\nabla \cdot V = 0 \tag{1}$$

$$\rho V \cdot \nabla V = -\nabla P + \mu \nabla^2 V \tag{2}$$
$$V \cdot \nabla C = D \nabla^2 C \tag{3}$$

$$V \cdot \nabla C = D \nabla^2 C \tag{3}$$

Where V, ρ , μ , and P are fluid velocity, density, dynamic viscosity, and pressure, respectively. Besides, C and D are the mass concentration of the species and the coefficient of diffusion of the fluids, respectively. In microscale flow, the Reynolds number is a significant dimensionless parameter. It is defined as follows [8]:

$$Re = \frac{\rho V d}{\mu} \tag{4}$$

Where d is the characteristic length of the flow field. To quantify mixing performance, the following equations were were employed [9]:

$$\sigma = \sqrt{\frac{1}{N} \cdot \sum_{i=1}^{N} (C_i - C_m)^2}$$
 (5)

$$\eta = 1 - \sqrt{\frac{\sigma^2}{\sigma_{max}^2}} \tag{6}$$

where, σ , σ_{max} , and η are the standard deviations of the mass fraction, the maximum variance of the mass fraction, and mixing efficiency, respectively. Besides, N, C_i , and C_m are the number of data points in a cross-sectional plane, the mass fraction of a point i, and the optimal mass fraction, respectively. The value $\eta=1$ represents completed mixing and $\eta=0$ corresponds to no mixing.

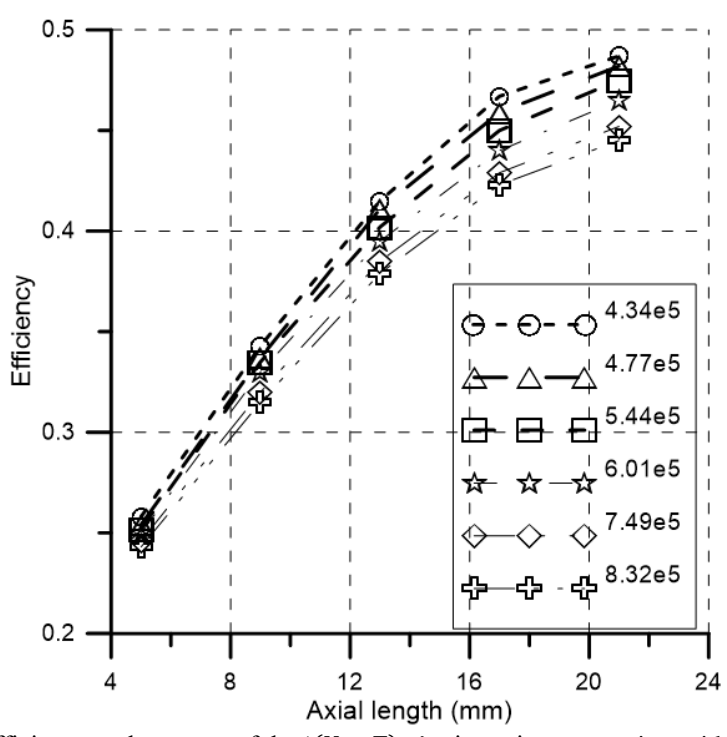


Fig. 3: Efficiency at the output of the ' $(Y - T)_0$ ' micromixer at varying grid numbers.

The CFD simulations were conducted using ANSYS Fluent version 15 commercial software. To ensure reliable and consistent numerical simulation results, each microchannel must have a grid-independent test. As an example, Figure 3 shows the grid independence test of $(Y - T)_{0}$ ° $(\alpha = 0)$ ° mixer for 6 different cell numbers. Efficiency decreases with the increase

of cell numbers as expected. Grid with $7.497.49 \times 10^6$ elements are chosen for further numerical simulation to reduce computational time and cost. A similar grid independence test is performed for all mixers.

To have a comprehensive analysis of both the mixing index and the associated pressure drop is imperative. The energy cost (MEC) is mathematically defined as the ratio of the input power to the mixing index and is a vital parameter for this study, mixing cost can be expressed as [10]:

Mixing Energy Cost (MEC) =
$$\frac{Input\ Power}{Mixing\ Efficiency} = \frac{\Delta P\ Q}{\eta}$$
 (7)

In equation (7), "input power" signifies the power needed to maintain the discharge (Q), while "mixing index" quantifies the degree of mixing achieved in the micromixer. This ratio provides a valuable metric for assessing the efficiency of the mixing process relative to the energy input.

4. Results and Discussion

In this study, a mixer containing Y and T segments is proposed, and optimized. Numerical computation was performed on the ' $(Y - T)_{\alpha}$ ' micromixers to analyze the effect of connecting angle α on the mixing of fluids and also to understand its impact on the dynamics of fluid flow inside the mixing channel throughout a spectrum of Reynolds numbers ranging from 1 to 100.

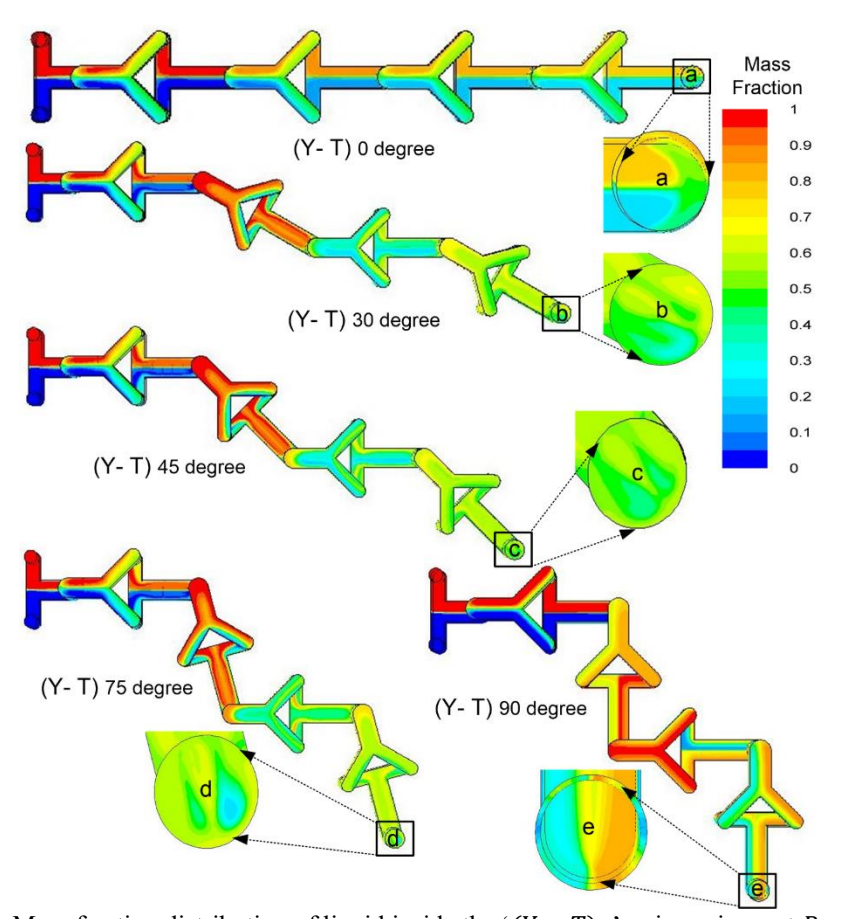


Fig. 4: Mass fraction distribution of liquid inside the ' $(Y - T)_{\alpha}$ ' micromixers at Re = 50.

Figure 4 shows the mass fraction distribution of fluids in a ' $(Y-T)_{\alpha}$ ' micromixer for Re=50. Red and blue colors colors represent two input fluids and contours express the mass fraction where green color (Mass fraction = 0.50) indicates indicates completer homogeneous mixing. The liquid gradually splits into several smaller layers as the flow continues inside inside the channels for all mixers. Thus, the inter-liquid interface area is enlarged, and the performance of the mixture is is improved. Among all mixers $(Y-T)_{45^{\circ}}$ shows the most homogeneous distribution at the output and $(Y-T)_{0^{\circ}}$ mixer shows the least homogeneity. Hence it is expected that $(Y-T)_{45^{\circ}}$ and $(Y-T)_{0^{\circ}}$ mixers will provide the highest and lowest mixing efficiency at Re=50, respectively.

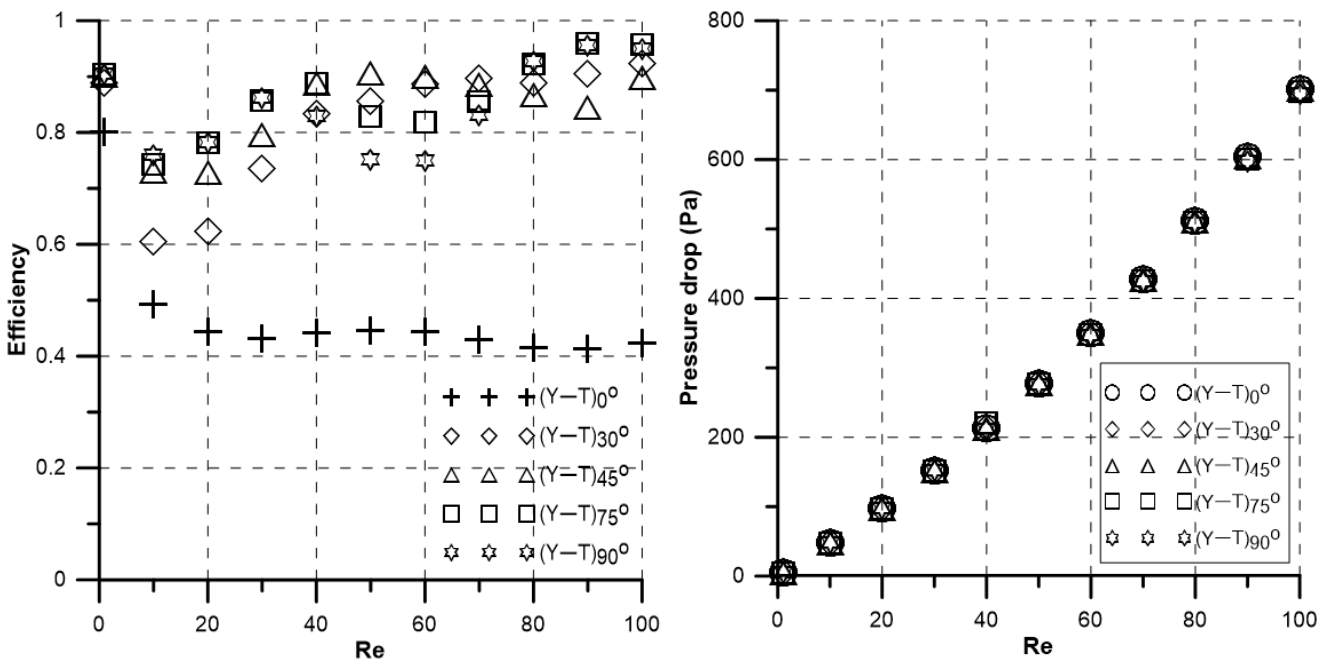


Fig. 5: (a) Variation of mixing efficiency (η) with Reynolds numbers 'Re' and (b) Variation of Pressure drop with Reynolds numbers 'Re'.

Figure 5 compares five designs in terms of mixing efficiency and required pressure drop at varying Reynolds numbers. All mixers show good efficiency at low velocity (Re=1) because the mixing time is large enough to mix the liquids due to molecular diffusion. In Figure 5a, $(Y-T)_{45^{\circ}}$ mixer demonstrates the best mixing efficiency at the mid-range of Reynolds number ($40 \le Re \le 80$) which is about 90%. At a higher Reynolds number ($Re \ge 80$) both $(Y-T)_{75^{\circ}}$ and $(Y-T)_{90^{\circ}}$ mixers exhibit efficiency greater than 93%. Among all presented mixers, $(Y-T)_{0^{\circ}}$ presents a poor mixing index (about 50%) at $Re \ge 10$. However, the required pressure drop shows negligible dependence on connecting angle α variation, as demonstrated in Figure 5b.

Figure 6 depicts the secondary flows after the 3rd element within the middle channel (YZ plane) of the proposed mixers at different Reynolds numbers. At Reynolds numbers equal to 10, all mixers behave uniformly with no noticeable secondary flow as indicated by the value of Helicity (H) and Vorticity(W_{yz}) in the yz plane. As the Reynolds number increases the influence of secondary flow is evident, all mixers show four counter-rotating vortices for at Re = 50 & 100. It is clear that $(Y - T)_{45^{\circ}}$ have a strong influence on secondary flow at Re = 50, ($H = 0.03 \ 1/s \& W_{yz} = 1.737 \ m/s^2$) which in turn influences the contact surface and causes the highest efficiency as shown in Figure 5a. On the other hand, at higher Reynolds

numbers, Re = 100, $(Y - T)_{75^{\circ}}$ and $(Y - T)_{90^{\circ}}$ mixers have strong secondary flow compared to other mixers, hence yielding an efficiency of more than 95%.

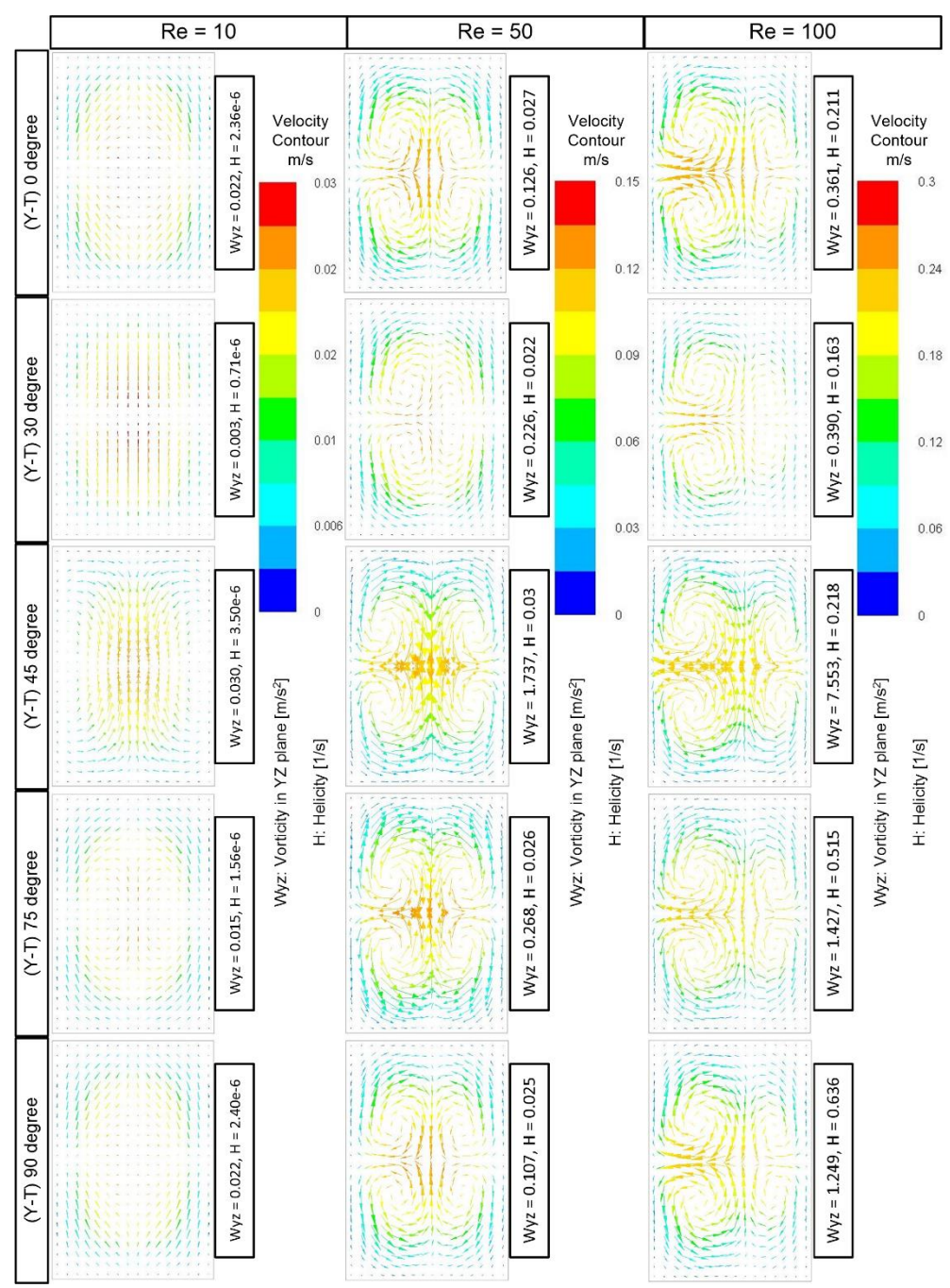


Fig. 6: Velocity vector on the Y-Z plane after third elements for different $(Y - H)_{\alpha}$ micromixers at Re = 10,50 & 100.

To have a comprehensive understanding of mixing performance it is important to consider the mixing energy cost (MEC). The MEC is calculated by taking into account variables like mixing index, pressure drop, and flow rate. To have a point of reference a well-known SAR Tear-drop mixer [11] is added. The MEC of SAR mixers is represented in Figure

7. The $(Y - T)_{0^{\circ}}$ mixer have the highest MEC due to high pressure drop and low mixing efficiency. whereas the lowest MEC is shown by $(Y - T)_{45^{\circ}}$ mixer which is significalty lower than the Tear-drop mixer.

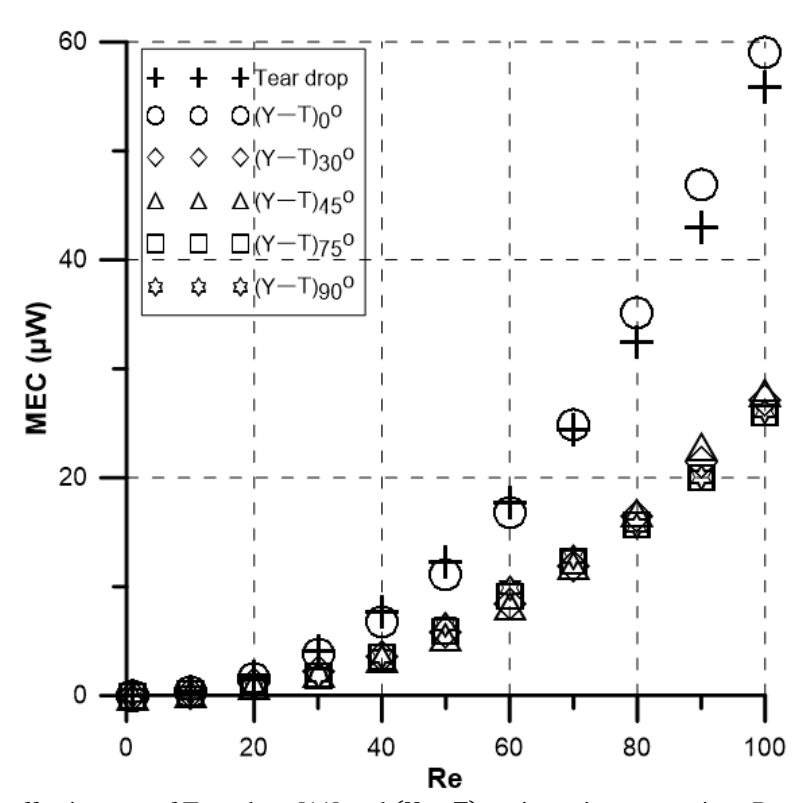


Fig. 7: Mixing effectiveness of Tear-drop [11] and $(Y - T)_{\alpha}$ micromixers at various Reynolds numbers.

4. Conclusion

A numerical assessment was conducted to investigate the mixing effectiveness of miscible fluids for a wide range of Reynolds numbers from 1 to 100. Based on a split-and-recombined mechanism, a novel mixer ' $(Y-T)_{\alpha}$ ' with 'Y' and 'T' shaped mixing units was designed. Ansys Fluent 15 commercial software was employed to analyze five mixers, denoted as $(Y-T)_{0^{\circ}}$, $(Y-T)_{30^{\circ}}$, $(Y-T)_{45^{\circ}}$, $(Y-T)_{75^{\circ}}$ and $(Y-T)_{90^{\circ}}$ at Reynolds number from 1 to 100. It is evident from numerical data, the SAR process strongly depends on angle α ; the weakest and the strongest effect can be seen at $\alpha=0^{\circ}$ and $\alpha=45^{\circ}$, respectively. In case of $(Y-T)_{\alpha}$ ' mixer, the mixing index is much higher for connecting angle $\alpha=45^{\circ}$ & 90° than $\alpha=0^{\circ}$. The reason is that, at this angle $(\alpha=0^{\circ})$, the strength of multi-lamination and secondary flow is much weaker compared to all other values of angle α . The mixing index is more than 90% for $(Y-H)_{45^{\circ}}$ for Reynolds numbers from 40 to 100. Mixing energy cost (MEC) is also computed for all ' $(Y-T)_{\alpha}$ ' and Tear-drop mixers. The mixer $(Y-T)_{45^{\circ}}$ shows favorable efficiency and MEC irrespective of Reynolds numbers.

Acknowledgments

Current work is sponsored by VC's Research Fund 2024. The authors would like to thank the Vice Chancellor of the IUB for supporting this work (VCRF-SETS:24-024).

References

- [1] M. Bayareh, M. N. Ashani, and A. Usefian, "Active and passive micromixers: A comprehensive review," *Chemical Engineering and Processing Process Intensification*, vol. 147. Elsevier B.V., Jan. 01, 2020, doi: 10.1016/j.cep.2019.107771.
- [2] A. Niculescu, C. Chircov, C. Alexandra, and A. M. Grumezescu, "Fabrication and Applications of Microfluidic Devices: A Review," pp. 1–26, 2021.
- [3] N. T. Nguyen and Z. Wu, "Micromixers A review," *Journal of Micromechanics and Microengineering*, vol. 15, no. 2. Feb. 2005, doi: 10.1088/0960-1317/15/2/R01.
- [4] B. Lee *et al.*, "Characterization of passive microfluidic mixer with a three-dimensional zig-zag channel for cryo-EM sampling," *Chem. Eng. Sci.*, vol. 281, p. 119161, Nov. 2023, doi: 10.1016/J.CES.2023.119161.
- [5] L. Capretto, W. Cheng, M. Hill, and X. Zhang, "Micromixing Within Microfluidic Devices," no. April, pp. 27–68, 2011, doi: 10.1007/128.
- [6] V. Hessel, H. Löwe, and F. Schönfeld, "Micromixers A review on passive and active mixing principles," *Chem. Eng. Sci.*, vol. 60, no. 8-9 SPEC. ISS., pp. 2479–2501, 2005, doi: 10.1016/j.ces.2004.11.033.
- [7] V. Viktorov, C. Visconte, and M. Readul Mahmud, "Analysis of a Novel Y-Y Micromixer for Mixing at a Wide Range of Reynolds Numbers," *J. Fluids Eng. Trans. ASME*, vol. 138, no. 9, pp. 1–9, 2016, doi: 10.1115/1.4033113.
- [8] G. Liu *et al.*, "A novel design for split-and-recombine micromixer with double-layer Y-shaped mixing units," *Sensors Actuators A Phys.*, vol. 341, no. March, p. 113569, 2022, doi: 10.1016/j.sna.2022.113569.
- [9] V. Viktorov, M. R. Mahmud, and C. Visconte, "Numerical study of fluid mixing at different inlet flow-rate ratios in Tear-drop and Chain micromixers compared to a new H-C passive micromixer," *Eng. Appl. Comput. Fluid Mech.*, vol. 10, no. 1, 2016, doi: 10.1080/19942060.2016.1140075.
- [10] B. Mondal, S. K. Mehta, P. K. Patowari, and S. Pati, "Numerical study of mixing in wavy micromixers: comparison between raccoon and serpentine mixer," *Chem. Eng. Process. Process Intensif.*, vol. 136, pp. 44–61, 2019, doi: 10.1016/j.cep.2018.12.011.
- [11] V. Viktorov, M. R. Mahmud, and C. Visconte, "Comparative analysis of passive micromixers at a wide range of Reynolds numbers," *Micromachines*, vol. 6, no. 8, pp. 1166–1179, 2015, doi: 10.3390/mi6081166.